We thank Charles Fierz and Mark Raleigh for their comments, which are reproduced in italic font below with responses in roman font.

Referee comments from Charles Fierz

the weakest point is the comparison of measurements with model simulations. While the scatter plots of Figure 10 may give the impression of a fair correlation between those two, a look at the supplementary material shows that there is still work to do. But one has to take in account that quantitative comparisons of simulations with measurements are still quite difficult to perform.
Indeed, there is much more work to do. This paper is about providing data necessary for that work, rather than directly about improving snow simulations. The simulations are included as an illustration of the data in use.

p. 1, line 11: Is "bulk" needed here? Snow depth and snow water equivalent are intrinsically related to the snow-cover as a whole anyway.
The word "bulk" is not needed in describing snow depth or snow water equivalent alone but is included here to emphasize the distinction between these measurements and vertically-resolved profile measurements.

p. 1, line 25: I wonder whether it would be better to cite the data set directly? WSL Institute for Snow and Avalanche Research SLF: Meteorological and snowpack measurements from Weissfluhjoch, Davos, Switzerland, Dataset, doi:10.16904/1, 2015
Done

p. 4, line 14: Equally important would be to know whether the instruments are ventilated.
The radiometers are mechanically ventilated but the temperature and humidity sensors are not.

p. 4, line 20: How far are AWS and radiometer tower apart? It may also be nice to mark the tower in Figure 1a.
They are 30 m apart, and are now marked on Figure 1b.

p. 5, line 25: Do you apply any undercatch correction to precipitation data? From Table 1 it also appears the height of the precipitation gauge is surprisingly low (1 m) compared to WMO standard (1.5 m). Is there a reason for it?
In fact, the precipitation data were taken from an optical gauge mounted at 2 m height to remain clear of the snow; this information has been corrected in Table 1 and added in the text. No wind correction is applied to the precipitation data, but wind speeds are generally low and the adjustment to match snow accumulation on the ground will correct any undercatch.

p. 7, line 3: The increase in longwave radiation does not seem to be that substantial given the canopy. Can you comment on that?
Snow measurements are made in a clearing but towards the shaded side where longwave radiation increases will be least. This is now discussed in more detail.

p. 7, lines 11-12: But wind adjustment will influence turbulent fluxes, will it not? Is this negligible?
The wind adjustment only makes a small difference in simulations with Crocus, but other models may be more sensitive. It is precisely because of the potential influence on turbulent fluxes that the wind adjustment is applied.

p. 7, line 17: Are turbulent fluxes at FMI-ARC never directed towards the snow cover?
This has been rephrased as "sensible and latent heat exchanges with the atmosphere" to avoid the impression that they are only in one direction.

p. 8, lines 20-21: 'supported on a stick' It would be nice to know how the thermistors are mounted though. Maybe you could cite another publication, as this paper is not the place to describe that design in detail. A photograph showing the depression in the snow cover could suffice too?
A link is now given to the page on the Sodankylä data archive for this system, which has photographs.

p. 8 line 25: The air will affect pit temperatures at all heights. Why is the base that different?
This has been rephrased as "digging a snow pit brings air into contact with snow beneath the surface".

p. 8, line 26: What volume? What cutter type is used?
Information that 250 and 500 cm^3 cutters are used and a reference (Leppänen et al. 2015, this volume) with more details have been added to the text.

Figure S1: Change 'density' to 'temperature' in caption
Done (and number corrected to S3)

Figures S1 S2: I'd label the ordinate (y-axis) as 'Height' rather than 'Snow depth', which is total snow height.
Done

Figures S1 S2: Reverse order in supplement
Corrected

***** NOTE: The name of Marie Dumont is misspelled in the author list appearing on the web

Referee comments from Mark Raleigh

- The driving and evaluation datasets are posted on the website of the Finnish Meteorological Institute (litdb.fmi.fi). What assurances are in place for long-term hosting of these data?
Under the open data policy of the Finnish Ministry of Transport and Communications, FMI is committed to the long-term upkeep and public distribution of its datasets. This assurance has been added to the text.

- It would be useful for future analyses of the forcing data if the meteorological datasets included flags indicating whether the data for each variable is original or filled at each time step (see Landry et al., 2014). Can you please include these flags?
A flag has been added to the forcing data files to record which variables had to be filled at each timestep, and this is now stated in the text.

- The posted datasets include most of the evaluation data (SWE, snow depth, temperature profiles) described but not all those found in Table 2. Will the other evaluation data (e.g., snowpit measurements of density and temperature) also be made available?
All of the datasets are listed on http://litdb.fmi.fi/index.php and are either directly available or available on request. It is now pointed out that contact information for each dataset is given in the database.

- *In the abstract, please state what years are included in the datasets.*
Done

- *In the modified dataset ('mod_2007-10-01_2014-09-30.csv'), there are four time steps on 11 April 2010 with negative shortwave values. Please correct these data.*
Corrected

- *In comparing the above and below canopy shortwave radiation, I found 1244 time steps where below canopy shortwave is greater than above canopy shortwave, which does not seem to make sense to me.*
We are very grateful to Dr Raleigh for spotting these data processing errors, which have been corrected. Fortunately, the corrections have had minimal impacts on snow simulations.

- *Please state the regularity with which the site is maintained/visited by FMI staff/technicians to check the integrity of instruments and check for measurement errors (e.g., snow on radiometer domes).*
Now stated in the text – the site is staffed 5 days a week and instruments are checked after every snowfall, when automatic error checking identifies a problem or at least 3 times a week.

- *Are the pyranometer and pyrgeometer heated/ventilated? Please clarify in the text.*
Clarified in the text – they are ventilated. Comparison of incoming and outgoing shortwave radiation suggests that unnoticed covering of the radiometers by snow is very rare.

- *Is the temperature sensor naturally ventilated or mechanically ventilated? Please clarify in the text.*
The text now states that the temperature sensor ventilation is natural.

- *Is the anemometer heated? Based on specifications, I think it is heated, but it would be good to state this in the text to allay concerns about freezing of the anemometer.*
Yes – now stated in the text

- *Pg. 2, Lines 22-25: Please consider including a reference to the Wayand et al. (2015) snow and meteorology dataset in the Washington Cascades as another recent example.*
Done

- *Pg. 3, Line 2: The FMI-ARC site is not only unique for being at a high latitude, but also at a low elevation (with snowfall temperatures close to 0 C, Pg. 6) and having a more shallow snowpack than the other snow sites with published datasets. It might be worth highlighting these distinct features.*
There are actually several mid-latitude continental sites of low relief with published snow data; the distinction of the FMI-ARC site is its high latitude.

- *Pg. 4, Line 2: A minor suggestion: it would be interesting to briefly summarize the data going back to 1908 and compare to the equivalent data summaries over the period represented in this dataset (Oct 2007 – Sept 2014). This would provide context, e.g., which years in this dataset had low/average/high precipitation in terms of the longer data record.*
A reference (Kivi et al. 1999) which includes a figure showing temperature changes since 1908 has been added. Statistics of annual maximum snow depth over 50 years have been added to provide context.

- *Pg. 5, Line 12: The supplement lists the ERA-Interim bias as -5.1 W/m2 (relative to observations). Please clarify whether any bias correction was applied to the ERAInterim data and why/why not.*
It is now explicitly stated that the bias has been removed.

- Pg. 5, Line 16: Please replace "Raleigh et al., 2015a" with "Raleigh et al., 2016" and update the citations in the references.
Done

- Pg. 6, Lines 2-10: Did this scale factor vary annually? Can you please specify the scale factor(s) here?
Annual scaling factors are now specified in a table.

- Pg. 6, Lines 24-25: There are potential problems with estimating canopy temperature from air temperature in some situations (see Webster et al., 2016). Please comment on this briefly.
This is now commented on as being more of a problem towards the sun-lit side of the clearing, and a reference on the issue (Pomeroy et al. 2009) has been added.

- Pg. 9, lines 26-28: Can you clarify whether the soils are freezing in these cases (as suggested by the observed soil temperatures)? Is anything known about the soil moisture?
A reference (Rautiainen et al. 2014) has been added showing that soil freezing can exceed 2 m in depth. It is now mentioned that soil moisture is measured but not used in this paper.

- Table 1: Air temperature and precipitation are both measured at 1 m. The maximum snow depth in the dataset is 1.02 m (late March 2010) and in five winters the maximum depth exceeds 0.80 m. Given spatial variability in snow depth, it begs the question whether the temperature sensor and precipitation gauge were ever buried in snow during the observational period. Please comment.
The air temperature and precipitation sensors are both mounted at 2 m height above the ground and have never been buried in snow.

- Table 1: Does the HMP35D measure temperature in addition to humidity? If so, was this used to double check and fill missing data from the PTB201A?
The HMP35D temperature output is not recorded.

- Figure 1: It would be helpful to include another panel with a map of Finland and a marker showing the site location in the country.
Done

- Figure 3b: The two lines are quite thin and difficult to distinguish to my eye. Can you please take some measures to help me discriminate them better?
The essential information in this figure is the mismatch between cumulated snowfall measurements and maximum SWE measured on the ground, so the red lines have been replaced by dots that show the cumulated snowfall up to the time of maximum SWE. There are no longer two lines that need to be distinguished.

- Figure 8: What depth are the soil temperature simulations / observations in this figure? Please clarify in the caption and/or figure.
Added to the caption

- Supplement: The caption of the third figure (multiple pages) with temperature profiles has two errors. First, the figure is called "Figure S1" when it should be "Figure S3". Second, the caption should state "Profiles of snow temperature" instead of "Profiles of snow density".
Corrected

Manuscript prepared for Geosci. Instrum. Method. Data Syst.
with version 2015/09/17 7.94 Copernicus papers of the LaTeX class copernicus.cls.
Date: 8 April 2016

A 7-year dataset for driving and evaluating snow models at an arctic site (Sodankylä, Finland)

Richard Essery[1], Anna Kontu[2], Juha Lemmetyinen[3], Marie Dumont[4], and Cécile B. Ménard[5]

[1]School of GeoSciences, University of Edinburgh, Edinburgh EH9 3FE, UK
[2]Arctic Research Unit, Finnish Meteorological Institute, 99600 Sodankylä, Finland
[3]Finnish Meteorological Institute, FI-00101 Helsinki, Finland
[4]Météo-France-CNRS, CNRM-GAME UMR 3589, CEN, Grenoble F-38000, France
[5]CORES Science and Engineering Ltd, Edinburgh, UK

Correspondence to: Richard Essery (richard.essery@ed.ac.uk)

Abstract. Datasets derived from measurements at Sodankylä, Finland, for driving and evaluating snow models are presented. This is the first time that such complete datasets have been made available for a site in the Arctic. The continuous October 2007 to September 2014 driving data comprise all of the meteorological variables required as inputs for physically-based snow models at hourly intervals: incoming solar and longwave radiation, snowfall and rainfall rates, air temperature, humidity, wind speed and atmospheric pressure. Two versions of the driving data are provided: one using radiation and wind speed measurements made above the height of the trees around the clearing where the evaluation data were measured and one with adjustments for the influence of the trees on conditions close to the ground. The available evaluation data include automatic and manual measurements of bulk snow depth and snow water equivalent, and profiles of snow temperature, snow density and soil temperature. A physically-based snow model is driven and evaluated with the datasets to illustrate their utility. Shading by trees is found to extend the duration of both modelled and observed snow cover on the ground by several days a year.

1 Introduction

Many studies have used meteorological data to drive snow models and meteorological or hydrological data to evaluate model performance at instrumented sites. These studies have often only used limited periods of driving data (e.g. two winters for several sites in Essery et al. (2009)) or limited evaluation data (e.g. infrequent manual measurements of snow mass in Slater et al. (2001)). Recently, valuable datasets have been published with multiple years of driving data and multiple sources of evaluation data for several snow research sites: Reynolds Mountain East in the Owyhee Mountains of Idaho (Reba et al., 2011), Col de Porte in the Chartreuse Mountains of France (Morin et al., 2012), the Senator Beck Basin in the San Juan Mountains of Colorado (Landry et al., 2014), Snoqualmie Pass in the Cascade Range of Washington (Wayand et al., 2015) and Weissflujoch in the Plessur

Alps of Switzerland (WSL, 2015). All of these are high-elevation, mid-latitude sites; there has been a lack of comparable datasets that could be used for evaluating snow models at high latitudes.

Snow models operating on energy balance principles form components of land surface models that are used to provide energy and moisture flux boundary conditions for the atmosphere in numerical weather prediction and climate models, but they can also be driven with measured meteorological data. The typical input data required are downwelling shortwave and longwave radiation fluxes, precipitation rate, air temperature, humidity, wind speed and atmospheric pressure. All of these variables can be measured with low-power instruments, but all are challenging to measure in cold and snowy environments where instruments can be covered by snow or ice and access for maintenance may be difficult. Model driving data have to be continuous, so gap filling is required if instrument or power failures occur. Data timesteps have to be somewhat shorter than a day (often 30 minutes or an hour) if situations in which snow melts during the day and refreezes at night are to be explicitly represented.

This paper presents model driving and evaluation datasets collated from measurements made at the Finnish Meteorological Institute's Arctic Research Centre (FMI-ARC) over the 7-year period starting on 1 October 2007. Descriptions are given of the site, instrumentation, gap filling used to construct a continuous driving dataset and adjustments of above-canopy measurements to allow for influences of shading by trees on below-canopy conditions. Comparisons of model simulations with evaluation data are presented as an illustration of data use and as a quality-control check on the data.

2 Site

FMI-ARC (67.368°N, 26.633°E, 179 m above sea level, Figure 1a) is collocated with the Sodankylä Geophysical Observatory beside the Kitinen river, 90 km north of the Arctic Circle and 7 km south-east of the town of Sodankylä in northern Finland. Snow typically lies from October until May; in daily records between 1951 and 2000, the annual maximum snow depth had a median of 83 cm, an interquartile range of 21 cm and a range from 62 cm (1954) to 119 cm (2000). Soil frost depths can reach over 2 m (Rautiainen et al., 2014) and air temperatures can fall below -30°C in winter, but the sun only remains entirely below the horizon for a few days in December. Continuous meteorological measurements have been made at or near this site since 1908 (Kivi et al., 1999). Current instrumentation includes an automatic weather station and an upper air sounding station (World Meteorological Organization index number 02836) which transmit data on the Global Telecommunication System for use by numerical weather prediction centres. In addition to regular measurement programmes, the Sodankylä area has been used in many remote sensing missions and field campaigns, including the Nordic Snow Radar Experiment (NoSREx), the Snow Reflectance Transition Experiment (SnoRTEx) and the Solid Precipitation Intercomparison Experiment (SPICE).

Figure 1b is an aerial orthophotograph of the site. The area around FMI-ARC is level and forested, predominantly with pine trees about 15 m tall, but many measurements are made in clearings or in a large wetland area to the east of the site. Driving data for this paper are taken from an automatic weather station (Figure 1c) and a radiometer tower (Figure 1d) 30 m apart, with instruments that are calibrated annually. Evaluation data are taken from an Intensive Observation Area (Figure 1e) that was established 590 m to the south of the weather station for NoSREx (Lemmetyinen et al., 2015). A list of many other observations not discussed in this paper and contact information can be found at http://litdb.fmi.fi/index.php.

3 Driving data and gap filling

All of the meteorological variables necessary for model driving are measured by the AWS and the radiometer tower at FMI-ARC with the instruments and at the heights listed in Table 1; note that radiation and wind measurements are made at heights above the forest canopy. The radiometers are ventilated and the anemometer is heated to reduce problems with freezing or snow accumulation, and instruments are cleaned after every snowfall or at least three times a week. Temperature and humidity sensors are naturally ventilated inside a Stevenson screen. Precipitation is measured using an optical sensor and two weighing gauges which give similar total amounts; data from the optical sensor are used here. There is no nearby wind speed measurement that could be used for gauge correction, but wind speeds are generally low and measured snowfall has been adjusted to match snow accumulation on the ground as described below. FMI-ARC is staffed five days a week, and automatic error checking can identify instrument problems immediately. For the 7-year period collated here, less than 1% of hourly data (visible as red points in Figure 2) are missing for any variable with the exception of longwave radiation; the longest period of missing data is a 52-day gap in the longwave radiation measurements from 10 September to 31 October 2011 because of a faulty power supply. The archived driving data files include a flag that records which data were missing and had to be filled for each hour.

Measurements from the AWS and the radiometer tower are used for driving data whenever they are available, but gaps have to be filled to form a complete driving dataset. Gaps of four hours or shorter are filled by linear interpolation. For shortwave radiation, air temperature, humidity and wind speed, longer gaps are filled with data from nearby instruments. No alternative longwave radiometer was operating at FMI-ARC for the full period, so longwave gaps are filled using ERA-Interim reanalyses (Dee et al., 2011). Longwave radiation fluxes in ERA-Interim are produced by short-range forecasts that can be expected to be accurate if the analysed vertical profiles of temperature and humidity in the atmosphere are accurate, although errors may be larger in cloudy conditions (Kangas et al., 2015). Data from both the surface synoptic station and the upper air station at Sodankylä are available for assimilation in reanalyses, and ERA-Interim compares well with the in situ measurements; the

longwave radiation measurements and forecasts have a correlation coefficient of 0.88 and a root mean square difference of 26.2 W m^{-2} after removal of a 5.1 W m^{-2} bias for periods when both are available (a scatter plot is included as supplementary material). Direct measurements of longwave radiation are rarely available for cold regions and snow models are known to be sensitive to longwave driving data (Raleigh et al., 2016); having near-continuous longwave measurements is therefore a distinct advantage of the FMI-ARC site.

Seven-year series of gap-filled hourly data are shown in Figure 2 for all of the driving variables apart from precipitation. Measuring solid precipitation is particularly challenging, and uncertainties in snowfall inputs are a major source of uncertainty in snow model outputs (Raleigh et al., 2015). Total precipitation is usually measured but has to be partitioned into snow and rain for mass balance calculations, either in the driving data or by the model. This is usually done by selecting a threshold or function of air temperature or wet-bulb temperature discriminating between rain and snow (Auer, 1974; Sims and Liu, 2015). Figure 3a shows the annual average snowfall partitioned from total precipitation for Sodankylä with varying temperature or wet-bulb temperature thresholds; the snowfall is not very sensitive to the choice of temperature or wet-bulb temperature as a predictor because humidity is usually high during precipitation, but it is sensitive to the choice of threshold because a significant amount of precipitation falls at temperatures close to 0°C. With precipitation classified as snow for temperatures lower than 2°C, Figure 3b shows that the cumulated amount of snowfall is less than the maximum observed snow water equivalent (SWE) on the ground in most winters but slightly greater in 2010-2011 and 2012-2013. Because the site is cold and little melting of snow occurs in autumn or winter, the cumulated snowfall should be close to the amount of snow on the ground at points that are not effected by canopy interception or wind redistribution. Snowfall data are therefore scaled by the factors required to match the maximum measured SWE each winter (Table 2); cumulated snowfall then also matches the rate of accumulation on the ground quite well, as shown in Figure 3b.

The snow measurement points in the IOA (Figure 2e) are not directly beneath trees, so snow accumulation there will not be greatly affected by canopy interception, but they are shaded from direct solar radiation by nearby trees. The presence of the trees will also increase the incoming longwave radiation and decrease the wind speed near the ground relative to more open locations. Measurements above the forest canopy height do not take these influences into account. To allow the use of snow models without representations of forest canopies, radiation fluxes and wind speed are adjusted in a modified driving dataset. From the hemispherical image of the canopy at the IOA in Figure 4a, the sky view fraction is estimated as f_v = 0.8 and a transmissivity τ for direct solar radiation is calculated by determining the fraction of each hour for which the sun would be blocked by the canopy. Modified solar radiation is given by

$$SW' = f_v SW_{dif} + \tau(SW - SW_{dif}), \quad (1)$$

where SW and SW_{dif} are the measured incoming global and diffuse solar radiation (Reid et al., 2014). Longwave radiation is modified by assuming that the canopy temperature can be approximated by the air temperature (Essery et al., 2008; Pomeroy et al., 2009) so that

$$LW' = f_v LW + (1 - f_v)\sigma T^4, \tag{2}$$

where LW is the measured incoming longwave radiation, $\sigma = 5.67 \times 10^{-8}$ W m^{-2} K^{-4} is the Stefan-Boltzmann constant and T is the air temperature in Kelvin. The resulting decreases in solar radiation and increases in longwave radiation are shown in Figure 4b. Solar and longwave radiation will both be underestimated by these modifications close to tree trunks at the sun-lit northern edge of the IOA clearing where the snow is observed to melt first.

An anemometer installed temporarily at 2 m height above the ground close to the IOA for 7 days in March 2012 recorded an average wind speed that was a fraction 0.35 of the wind speed at 22 m height (equal to the ratio given by a logarithmic wind profile with a roughness length of 0.55 m). This ratio is used to scale the wind speed in the modified driving data set. There is no permanently installed anemometer below the canopy height at the IOA, so the wind adjustment is highly uncertain. Because the wind is rarely strong enough to move snow in the IOA and snowmelt is dominated by radiation in spring, however, it is expected that models will not be highly sensitive to the wind adjustment.

4 Evaluation data

Physically-based snow models may include snow temperature, mass, density, liquid water content and grain size in layers as state variables. Predicted fluxes will include reflected shortwave radiation, emitted longwave radiation, sensible and latent heat exchanges with the atmosphere, and conducted heat flux and drainage of water at the base of the snowpack. Snow properties that have to be predicted include albedo and thermal conductivity. Measurements of any state variable, flux or property may be used as evaluation data for models, and the measurements need not be continuous; measured and modelled variables can be compared at whatever times for which measurements are available.

FMI-ARC data that will be used in the model evaluation below are listed in Table 3. Again, many more measurements are made in the IOA in addition to those discussed here, including snow grain size, hardness, wetness and microwave brightness temperatures, and soil moisture. The microstructure of snow samples taken during special experiments has been measured in great detail by X-ray computed tomography (Proksch et al., 2015). Outgoing radiative and turbulent flux measurements are made above the canopy height at FMI-ARC, so they would be most useful for evaluating models that include vegetation canopies.

Snow depth and SWE are measured in the IOA both manually about once a week and many times daily with automatic instruments. These measurements are compared in Figure 5. The output of the experimental SWE sensor, which works by measuring the attenuation of gamma radiation from a

source beneath the snow, is noisy but tracks the manual measurements well after calibration and averaging. Snow accumulation varies spatially. Figure 6 compares the snow depth in the IOA for the winter of 2012-2013 with snow depths measured in the forest beside the IOA and 900 m to the northeast on the wetland. The snow was deepest throughout the winter and melted latest in the IOA. Some snow is intercepted by the forest canopy as it falls and can sublimate, reducing the depth of snow on the forest floor. Wind can remove and compact snow in the open wetland area, again reducing the snow depth. Differences in snow accumulation and melt rates lead to differences in the persistence of snow cover at different sites; the measured snow depth fell to zero on 3 May 2013 on the wetland, 6 May in the forest and 13 May in the IOA. Photographs of the IOA in Figure 7 show small-scale variations in cover as the snow melts. Bare patches first appear around the bases of trees, and the snow lies longest at the shady side of the clearing.

Snow temperatures are measured continuously by an array of thermistors supported on a stick that becomes buried in the snow (http://litdb.fmi.fi/ioa0007_data.php) and intermittently by inserting a stem thermometer into the snow face when pits are dug. Both methods are subject to biases; it has been observed that the thermistor stick interferes with the accumulation of snow and can form a depression up to 30 cm deep in the snow surface, and digging a snow pit brings air into contact with snow beneath the surface. Density is measured by weighing 250 or 500 cm^3 snow samples cut from snow pits (Leppänen et al., 2015) and also by a dielectric method that relates density and wetness to the measured permittivity of snow (Sihvola and Tiuri, 1986). The dielectric method generally gives lower densities than gravimetric sampling of snow at Sodankylä.

5 Model results

Preliminary versions of the driving and evaluation datasets were used in a study with the JULES land surface model by Ménard et al. (2015). The above-canopy and modified driving datasets are used here to drive Crocus (Vionnet et al., 2012), which is a detailed multi-layer snowpack model originally developed for avalanche forecasting in the French mountains. Although physically-based, some of the processes in Crocus have been parametrized using experimental results from the mid-latitude site at Col de Porte (45.3°N, 5.8°E, 1325 m a.s.l.), which is much warmer than Sodankylä in winter and has heavier snowfall.

Figure 8 compares Crocus simulations driven by the above-canopy and below-canopy datasets with measurements of snow depth, SWE and soil temperature. Simulated snow depths are generally close to the measurements but are sometimes overestimated after snowfall because of Crocus predicting densities for fresh snow that are lower than observed at Sodankylä. Simulated SWE follows the measurements during the accumulation periods, which is to be expected because of the lack of mid-winter melt and the scaling of the snowfall in the driving data to the SWE measurements. Snowmelt starts at about the right time each spring in the simulations but then proceeds faster than

observed. The modified driving data reduces melt rates; simulations with the above-canopy driving data remove the snow on average 13 days earlier than the snow disappearance dates inferred from the ultrasonic depth gauge at the IOA, but simulations with the modified below-canopy driving data remove the snow on average only 6 days earlier than observed. As shown by Figure 7, the dates of snow disappearance can differ by two weeks even over short distances in reality; this spatial variability is not represented by a one-dimensional model such as Crocus. Simulated soil temperatures have cold spikes that are greater than observed at the start of some winters but then remain close to 0°C once the snowpack has become established. Measured soil temperatures also show a strong influence of insulation by snow but can fall a couple of degrees lower than the simulations in late winter.

The frequent snow pit measurements in the IOA and the multi-layer outputs of Crocus give a large amount of data for comparison. Profiles of temperature and density for 140 snow pits dug between 7 December 2009 and 14 May 2014 are plotted in a supplement, but the evolution of the snowpack over the winter of 2012-2013 alone is shown in Figure 9. Snow pits were dug once a week, usually on Tuesday but sometimes on Wednesday or Thursday, for the 28 weeks between 31 October 2012 and 7 May 2013. Simulations and measurements both show temperatures remaining close to 0°C at the base of the snowpack with periods of much colder temperatures in snow layers close to the surface. The snow then rapidly warms and becomes wet and isothermal at 0°C when melt begins in spring. Density generally increases with depth in the snowpack and with time, again increasing rapidly once the snow becomes wet.

Quantitative comparisons between simulated and measured profiles of snow properties are complicated by differences in simulated and measured snow depths. Simply making scatter plots (Figure 10) of variables at the same heights above the ground and at the same times shows strong correlations of 0.80 between simulated and measured snow temperatures and 0.74 for densities. The simulated temperatures tend to be higher than observed for the warmer temperatures found near the base of the snowpack.

6 Conclusions

Data from the FMI Arctic Research Centre at Sodankylä have been used to construct datasets that will allow driving of snow models for multiple years and evaluation of model outputs against multiple types of observations. There are some gaps in the data, but the availability of additional instruments and high-quality atmospheric reanalyses give confidence in the filling of gaps to provide continuous driving data. The utility of the datasets has been demonstrated by driving the Crocus snow model and evaluating its outputs against snow depth, SWE, snow density, snow temperature and soil temperature measurements. The physical basis of the model allows it to perform well in an arctic environment very different to the mid-latitude mountain environments for which it was first developed.

It is intended that Sodankylä will be used as a reference site in an upcoming evaluation of snow simulations in Earth System models (http://www.climate-cryosphere.org/activities/targeted/esm-snowmip). Under the open data policy of the Finnish Ministry of Transport and Communications, FMI is committed to the long-term upkeep and public distribution of its data; the datasets used in this paper can be downloaded from the FMI litdb archive at http://litdb.fmi.fi/ESMSnowMIP.php.

Acknowledgements. The staff at FMI-ARC are thanked for data collection and maintenance of instruments. Collection of evaluation data in the IOA was supported by ESA ESTEC contract 22671/09/NL/JA/ef. Visits to FMI-ARC by the first author were supported by NERC grant NE/H008187/1 and ESA ESTEC contract 23103/09/NL/JC. Samuel Morin and Matthieu Lafaysse assisted with the Crocus simulations. The orthophotograph in Figure 1b was supplied by the Finnish Geospatial Research Institute. We are grateful to Charles Fierz and Mark Raleigh for their helpful comments in reviewing this paper.

References

Auer, A. H.: The rain versus snow threshold temperatures, Weatherwise, 27, 67, 1974.

Dee, D. P., S. M. Uppala, A. J. Simmons, P. Berrisford, P. Poli, S. Kobayashi, U. Andrae, M. A. Balmaseda, G. Balsamo, P. Bauer, P. Bechtold, A. C. M. Beljaars, L. van de Berg, J. Bidlot, N. Bormann, C. Delsol, R. Dragani, M. Fuentes, A. J. Geer, L. Haimberger, S. B. Healy, H. Hersbach, E. V. Hólm, L. Isaksen, P. Kallberg, M. Köhler, M. Matricardi, A. P. McNally, B. M. Monge-Sanz, J.-J. Morcrette, B.-K. Park, C. Peubey, P. de Rosnay, C. Tavolato, J.-N. Thépaut and F. Vitart: The ERA-Interim reanalysis: configuration and performance of the data assimilation system, Q. J. R. Meteorol. Soc., 137, 553-597, doi:10.1002/qj.828, 2011.

Essery, R. L. H., J. Pomeroy, C. Ellis and T. Link: Modelling longwave radiation to snow beneath forest canopies using hemispherical photography or linear regression, Hydrol. Processes, 22, 2788-2800, 2008.

Essery, R., N. Rutter, J. Pomeroy, R. Baxter, M. Stähli, D. Gustafsson, A. Barr, P. Bartlett and K. Elder: SnowMIP2: An evaluation of forest snow process simulations, Bull. Amer. Meteor. Soc., 90, doi:10.1175/2009BAMS2629.1, 2009.

Kangas, M., L. Rontu, C. Fortelius, M. Aurela and A. Poikonen: Weather model verification using Sodankylä mast measurements, Geosci. Instrum. Method. Data Syst. Discuss., 5, 577-598, doi:10.5194/gid-5-577-2015, 2015.

Kivi, R., E. Kyrö, T. Turunen, T. Ulich and E. Turunen: Atmospheric trends above Finland. Part II. Troposphere and stratosphere, Geophysica, 35, 71-85, 1999.

Landry, C. C., K, A. Buck, M, S. Raleigh and M. P. Clark: Mountain system monitoring at Senator Beck Basin, San Juan Mountains, Colorado: A new integrative data source to develop and evaluate models of snow and hydrologic processes, Water Resour. Res., 50, 1773-1788, doi:10.1002/2013WR013711, 2014.

Lemmetyinen, J., A. Kontu, J. Pulliainen, J. Vehviläinen, K. Rautiainen, A. Wiesmann, C. Mätzler, C. Werner, H. Rott, T. Nagler, M. Schneebeli, M. Proksch, D. Schüttemeyer, M. Kern and M. Davidson: Nordic Snow Radar Experiment, Geosci. Instrum. Method. Data Syst. Discuss., doi:10.5194/gi-2015-29, 2015.

Leppänen, L., A. Kontu, H.-R. Hannula, H. Sjöblom and J. Pulliainen: Sodankylä manual snow survey program, Geosci. Instrum. Method. Data Syst. Discuss., 5, 405-426, doi:10.5194/gid-5-405-2015, 2015.

Ménard, C. B., J. Ikonen, K. Rautiainen, M. Aurela, A. N. Arslan and J. Pulliainen: Effects of meteorological and ancillary data, temporal averaging, and evaluation methods on model performance and uncertainty in a land surface model, J. Hydrometeorol., 16, 2559-2576, doi: 10.1175/JHM-D-15-0013.1, 2015.

Morin, S., Y. Lejeune, B. Lesaffre, J.-M. Panel, D. Poncet, P. David and M. Sudul: An 18-yr long (1993-2011) snow and meteorological dataset from a mid-altitude mountain site (Col de Porte, France, 1325m alt.) for driving and evaluating snowpack models, Earth Syst. Sci. Data, 4, 13-21, doi:10.5194/essd-4-13-2012, 2012.

Pomeroy, J.W., D. Marks, T. Link, C. Ellis, J. Hardy, A. Rowlands and R. Granger: The impact of coniferous forest temperature on incoming longwave radiation to melting snow Hydrol. Processes, 23, 2513-2525, 10.1002/hyp.7325, 2009

Proksch, M., H. Löwe and M. Schneebeli: Density, specific surface area, and correlation length of snow measured by high-resolution penetrometry, J. Geophys. Res. Earth Surf., 120, 346-362, doi:10.1002/2014JF003266, 2015.

Raleigh, M. S., J. D. Lundquist and M. P. Clark: Exploring the impact of forcing error characteristics on physically based snow simulations within a global sensitivity analysis framework, Hydrol. Earth Syst. Sci., 19, 3153-3179, doi:10.5194/hess-19-3153-2015, 2015.

Raleigh, M. S., B. Livneh, K. Lapo and J. D. Lundquist: How does availability of meteorological forcing data impact physically-based snowpack simulations? J. Hydrometeorol., 17(1), 99-120, doi:10.1175/JHM-D-14-0235.1, 2016.

Rautiainen, K., J. Lemmetyinen, M. Schwank, A. Kontu, C. B. Ménard, C. Mätzler, M. Drusch, A. Wiesmann, J. Ikonen, J. Pulliainen: Detection of soil freezing from L-band passive microwave observations, Remote Sens. Environ., 147, 206-218, doi:10.1016/j.rse.2014.03.007, 2014.

Reba, M. L., D. Marks, M. Seyfried, A. Winstral, M. Kumar and G. Flerchinger: A long-term data set for hydrologic modeling in a snow-dominated mountain catchment, Water Resour. Res., 47, doi:10.1029/2010WR010030, 2011.

Reid, T.D., R. L. H. Essery, N. Rutter and M. King: Data-driven modelling of shortwave radiation transfer to snow through boreal birch and conifer canopies, Hydrol. Processes, 28, 2987-3007, doi:10.1002/hyp.9849, 2014.

Sihvola, A., and M. Tiuri: Snow Fork for field determination of the density and wetness profiles of a snow pack, IEEE Trans. Geosci. Remote Sens., 5, 717-721, 1986

Sims, E. M., and G. Liu: A Parameterization of the probability of snow-rain transition, J. Hydrometeorol., 16, 1466-1477, doi:http://dx.doi.org/10.1175/JHM-D-14-0211.1, 2015.

Slater, A. G., and 32 others: The representation of snow in land surface schemes: results from PILPS 2(d), J. Hydrometeorol., 2, 7-25, 2001.

Vionnet, V., E. Brun, S. Morin, A. Boone, S. Faroux, P. Le Moigne, E. Martin and J.-M. Willemet: The detailed snowpack scheme Crocus and its implementation in SURFEX v7.2, Geosci. Model Dev., 5, 773-791, doi:10.5194/gmd-5-773-2012, 2012.

Wayand, N. E., A. Massmann, C. Butler, E. Keenan, J. Stimberis and J. D. Lundquist: A meteorological and snow observational data set from Snoqualmie Pass (921 m), Washington Cascades, USA, Water Resour. Res., 51, 10092-10103, doi:10.1002/2015WR017773, 2015.

WSL Institute for Snow and Avalanche Research SLF: Meteorological and snowpack measurements from Weissfluhjoch, Davos, Switzerland, Dataset, doi:10.16904/1, 2015.

Table 1. Instruments and missing data for meteorological driving variables between 1 October 2007 and 30 September 2014

Variable	Instrument	Height	Missing data
Precipitation	Vaisala FD12P	2 m	0.67%
Air pressure	Vaisala PTB201A	1 m	0.11%
Air temperature	Pentronic PT100	2 m	0.11%
Relative humidity	Vaisala HMP35D	2 m	0.19%
Global solar radiation	Kipp & Zonen CM11	14 m	0.61%
Diffuse solar radiation	Kipp & Zonen CM11 with shading ball	14 m	0.55%
Longwave radiation	Kipp & Zonen CG4	14 m	8.65%
Wind speed	Vaisala WAA25	22 m	0.12%

Table 2. Scaling factors required to match measured snowfall to measured snow accumulation

Winter	Factor
2007-2008	1.373
2008-2009	1.165
2009-2010	1.131
2010-2011	0.922
2011-2012	1.093
2012-2013	0.971
2013-2014	1.092

Table 3. Evaluation data from the IOA

Variable	Instrument
Snow depth	Campbell Scientific SR50 Manual sampling
Snow water equivalent	Astrock Gamma Water Instrument Manual sampling
Snow density profiles	Toikka Snow Fork sampling at 10 cm height increments from 9/10/2009 Manual sampling at 5 cm height increments from 7/12/2009
Snow temperature profiles	Campbell Scientific 107-L at 10 cm height increments from 6/9/2011 Manual sampling at 10 cm height increments
Soil temperature profiles	Decagon Devices 5TE at 5, 10, 20, 40 and 80 cm depths from 6/9/2011

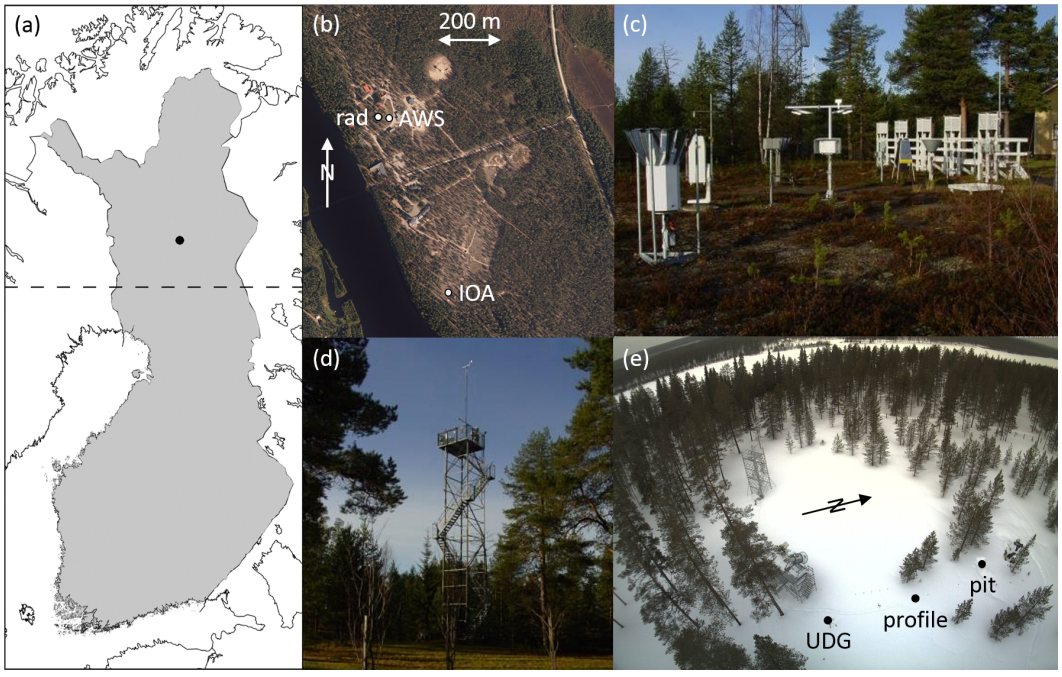

Figure 1. (a) The location of FMI-ARC (dot), 90 km north of the Arctic Cirle (dashed line) in Finland. (b) Orthophotograph of the FMI-ARC site, showing the locations of the automatic weather station (AWS), the radiometer tower (rad) and the Intensive Observation Area (IOA). (c) The automatic weather station, with the radiometer tower in the background. (d) The radiometer tower. (e) The IOA, showing the locations of the ultrasonic depth gauge (UDG), the snow temperature profile and the snow pit for manual measurements.

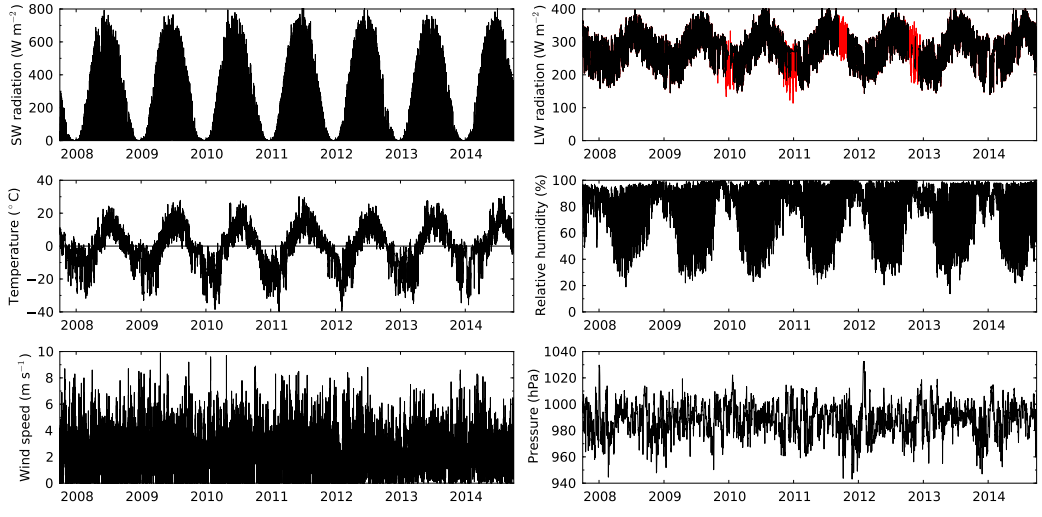

Figure 2. Hourly timeseries of shortwave radiation, longwave radiation, air temperature, relative humidity, wind speed and pressure. Longwave radiation data points in red are from reanalyses.

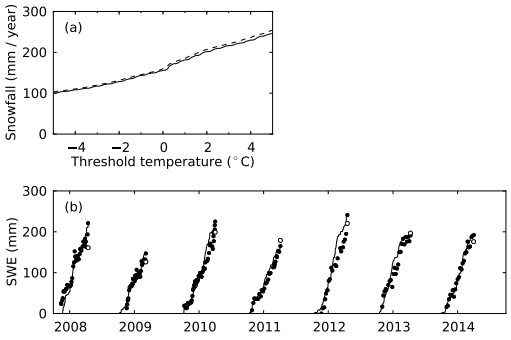

Figure 3. (a) Average annual snowfall derived from total precipitation with varying temperature (solid line) or wet-bulb temperature (dashed line) thresholds. (b) SWE on the ground from manual observations up to the maximum each winter (black dots), cumulated snowfall up to the date of maximum SWE (white dots) and snowfall scaled to the annual maxima (black lines).

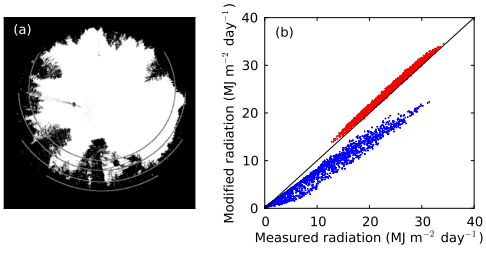

Figure 4. (a) A hemispherical photograph taken close to the IOA snow depth sensor in August 2011, showing the track of the sun (grey lines) on the first days of February, March, April and May. (b) Measured above-canopy and modified below-canopy daily solar (blue points) and longwave (red points) radiation.

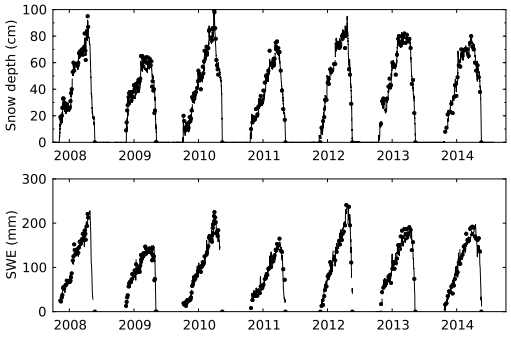

Figure 5. Measured snow depth and SWE from manual measurements (dots) and automatic instruments (lines). Daily averages of the automatic SWE measurements are used to reduce noise.

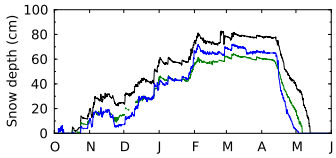

Figure 6. Snow depths measured in the IOA (black line), in the forest (green line) and on the wetland (blue line) for the winter of 2012-2013.

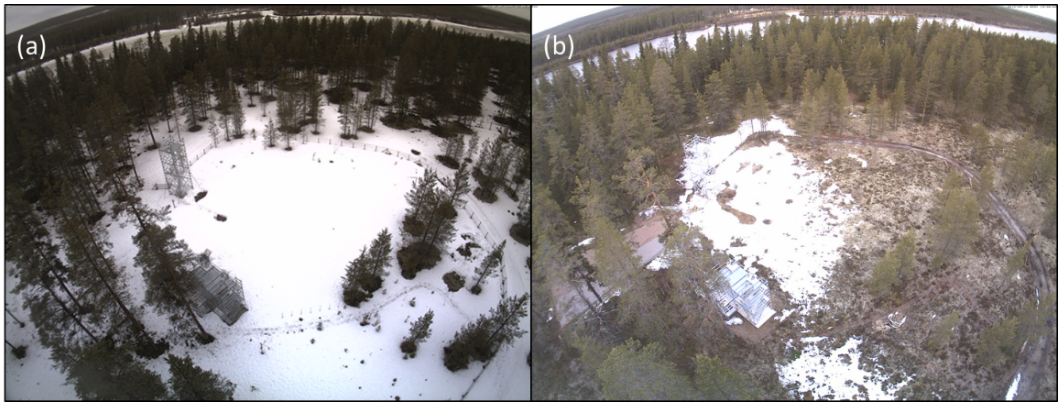

Figure 7. Snow melting in the IOA at noon on (a) 1 May and (b) 13 May 2013.

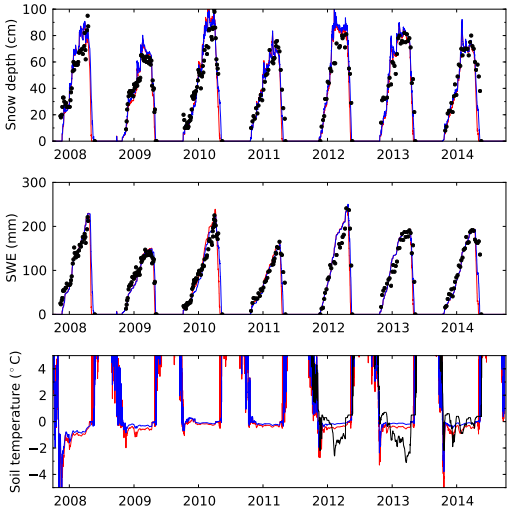

Figure 8. Crocus simulations with the above-canopy (red lines) and below-canopy (blue lines) driving datasets, compared with measurements (black dots and lines) of snow depth, SWE and soil temperature at 10 cm depth. For clarity, only manual measurements of snow depth and SWE are shown.

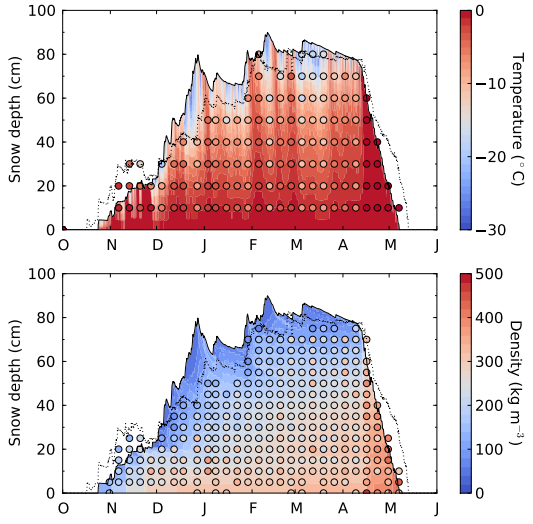

Figure 9. Profiles of snow temperature and density from Crocus simulations (background colours) and snow pit measurements (coloured dots) for the winter of 2012-2013. Dotted lines show the measured snow depth.

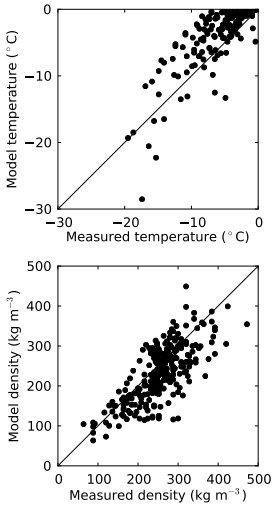

Figure 10. Scatter plots of Crocus simulations and manual snow pit measurements of snow temperature and density for the winter of 2012-2013.

A 7-year dataset for driving and evaluating snow models at an arctic site (Sodankylä, Finland)

Richard Essery, Anna Kontu, Juha Lemmetyinen, Marie Dumont and Cécile B Ménard

Supplementary figures

Figure S1. Scatter plot and statistics comparing in situ measurements and ERA-Interim forecasts of longwave radiation averaged over periods of 3 hours (blue dots) and a day (red dots).

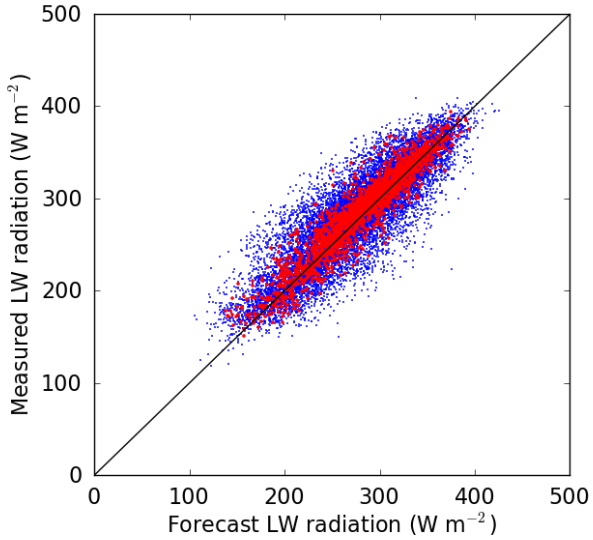

Period	Bias (W m^{-2})	Root mean square error (W m^{-2})	Correlation
3 hours	-5.1	26.7	0.88
24 hours	-5.1	16.9	0.94

Figure S2. Profiles of snow density from manual measurements (black dots), dielectric measurements (white dots) and Crocus simulations (lines).

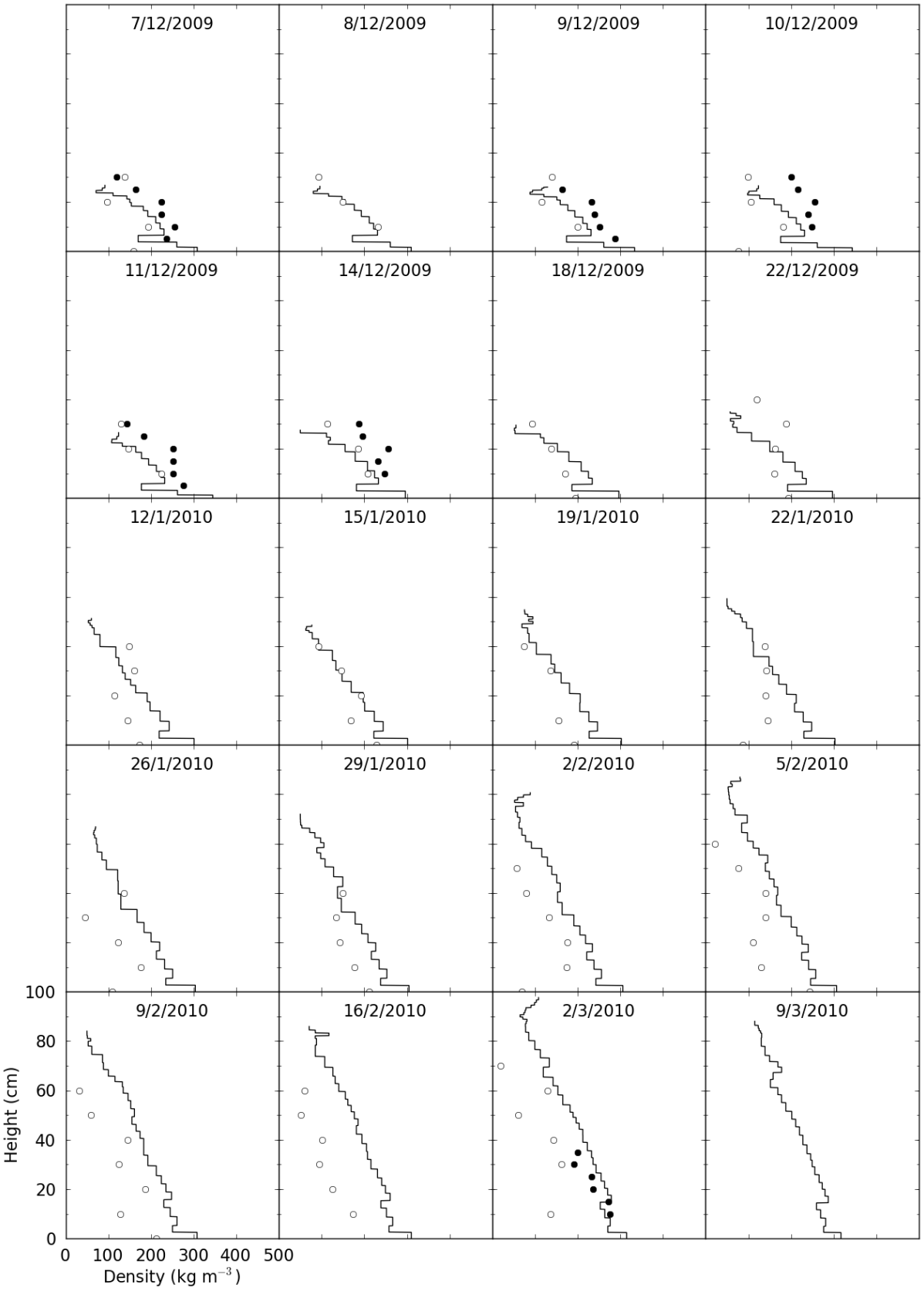

Figure S2. Continued

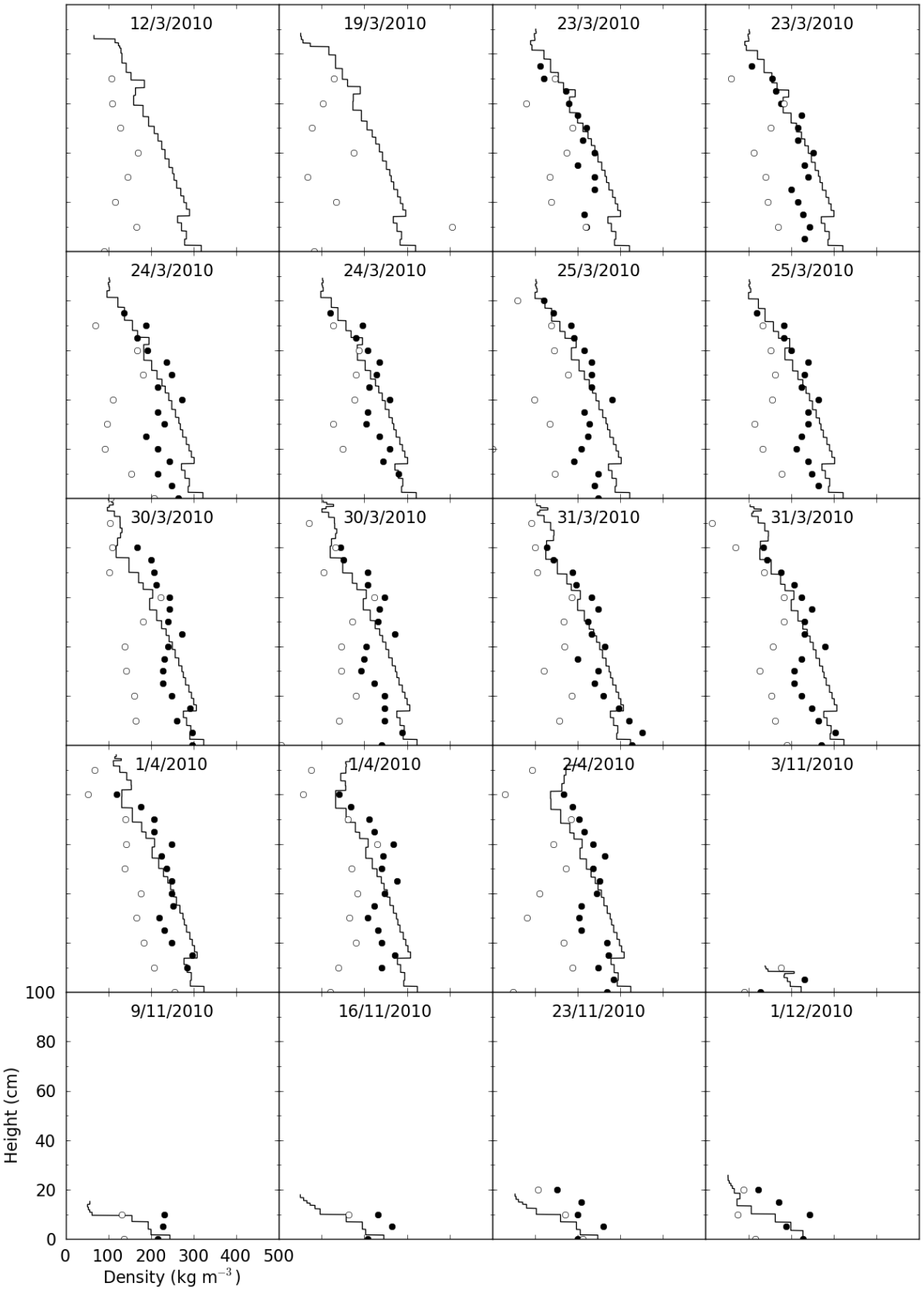

Figure S2. Continued

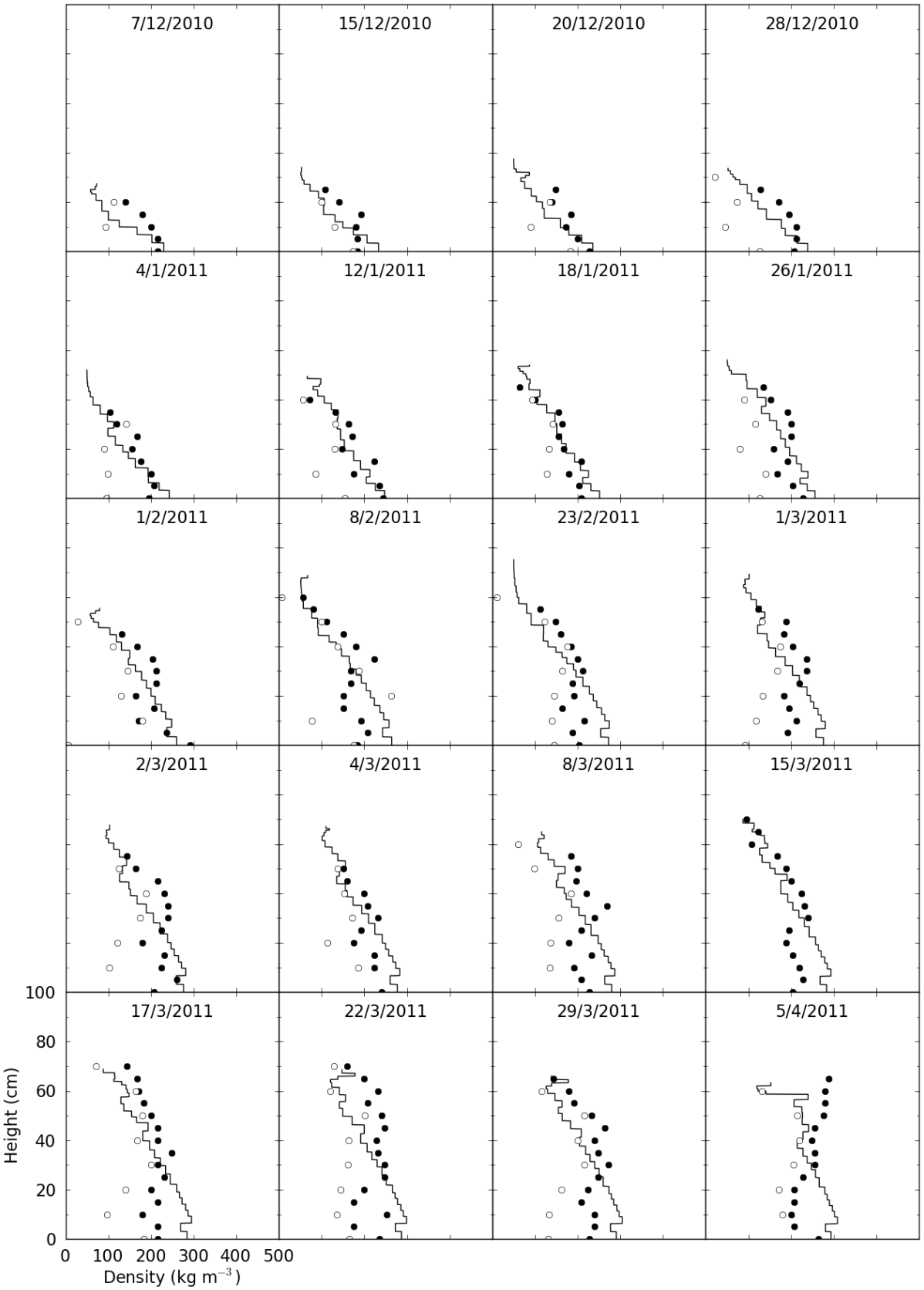

Figure S2. Continued

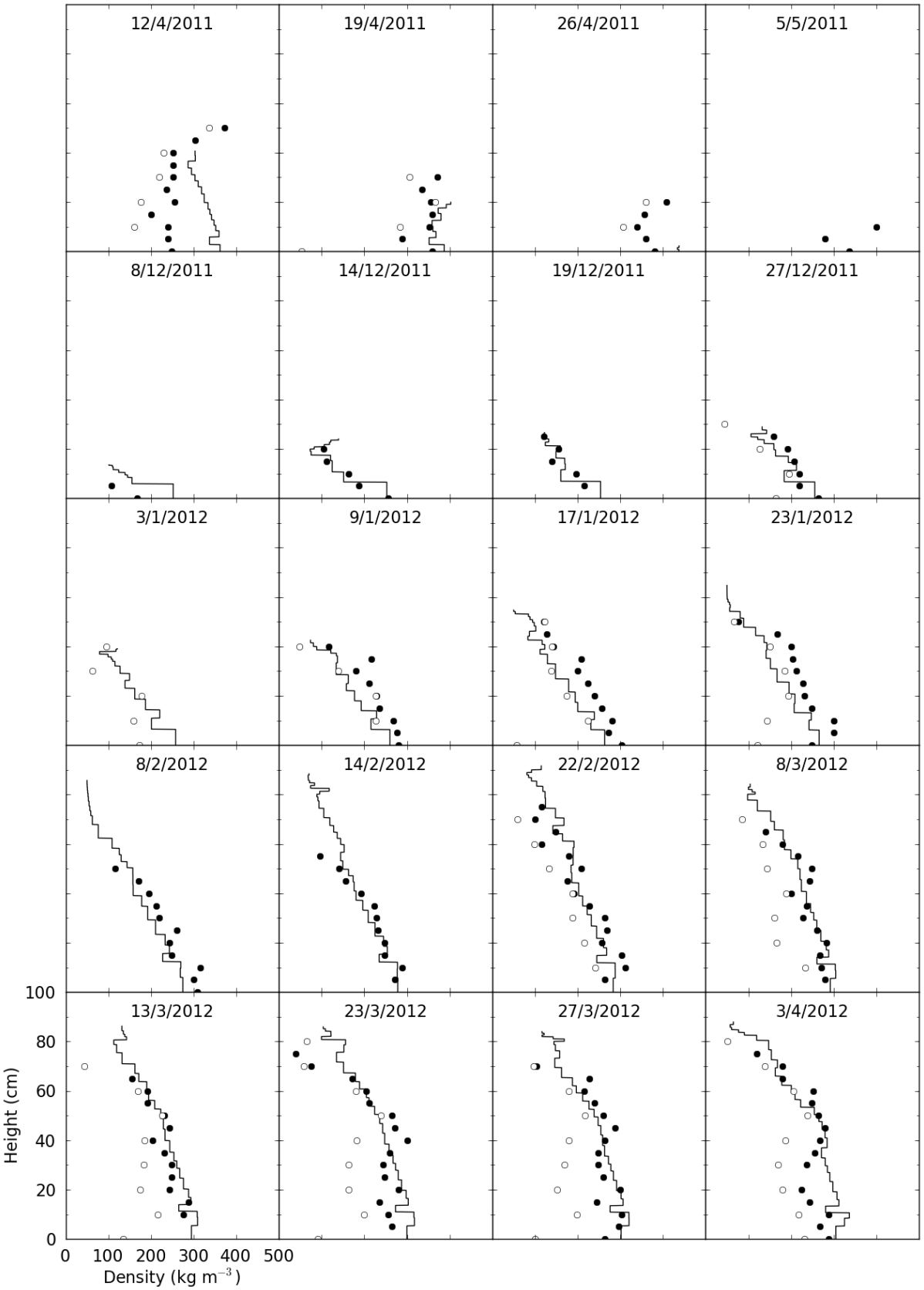

Figure S2. Continued

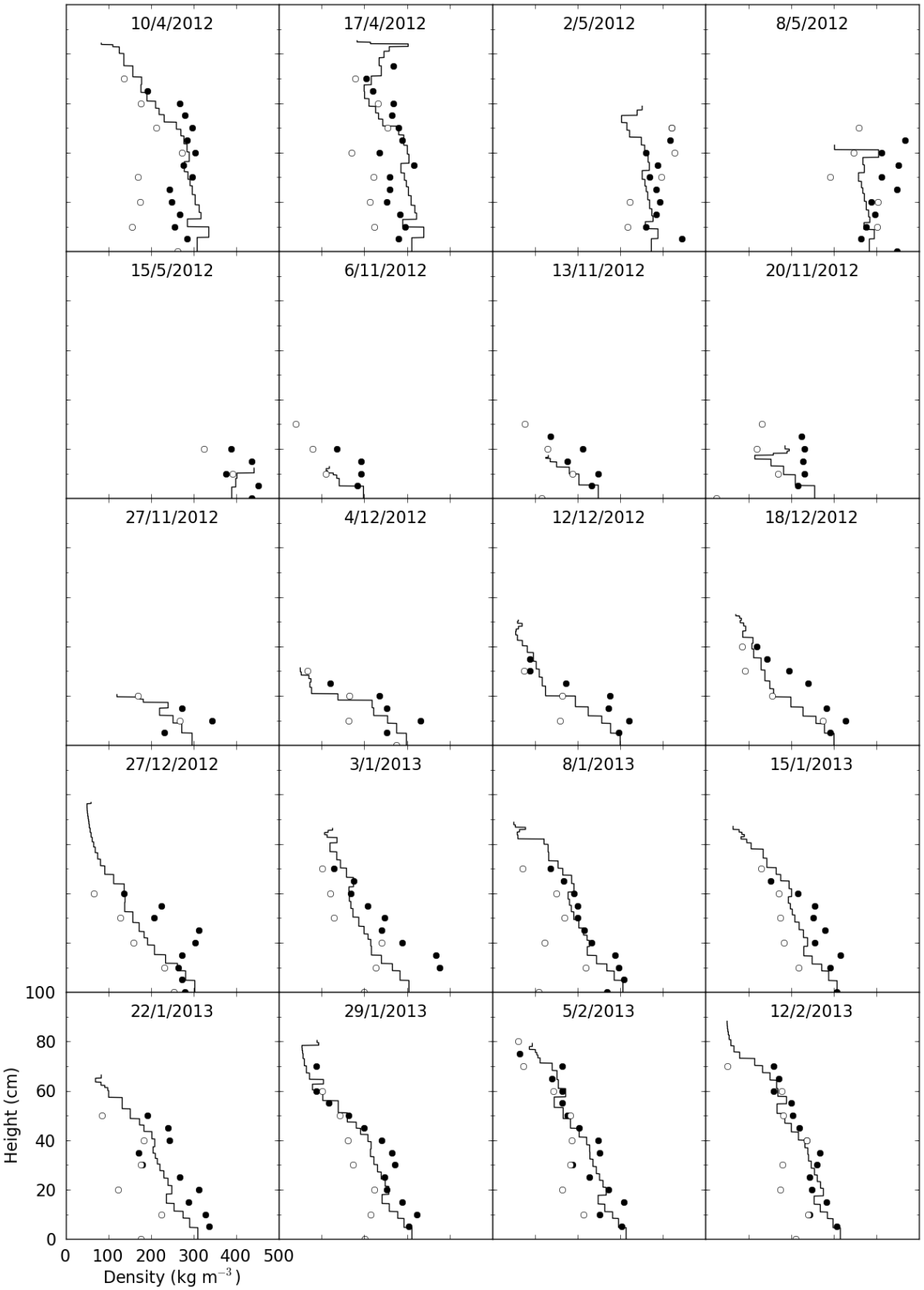

Figure S2. Continued

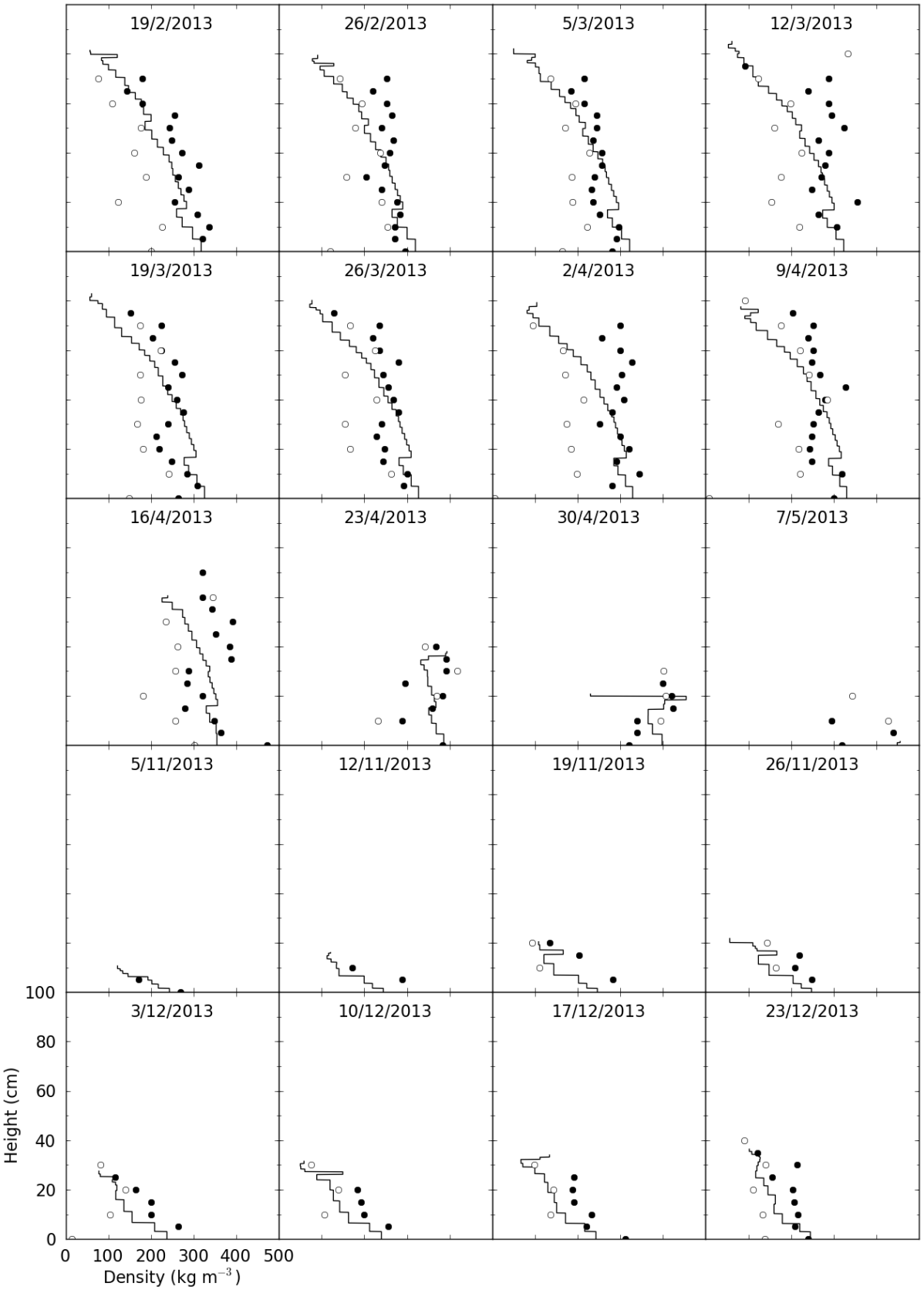

Figure S2. Continued

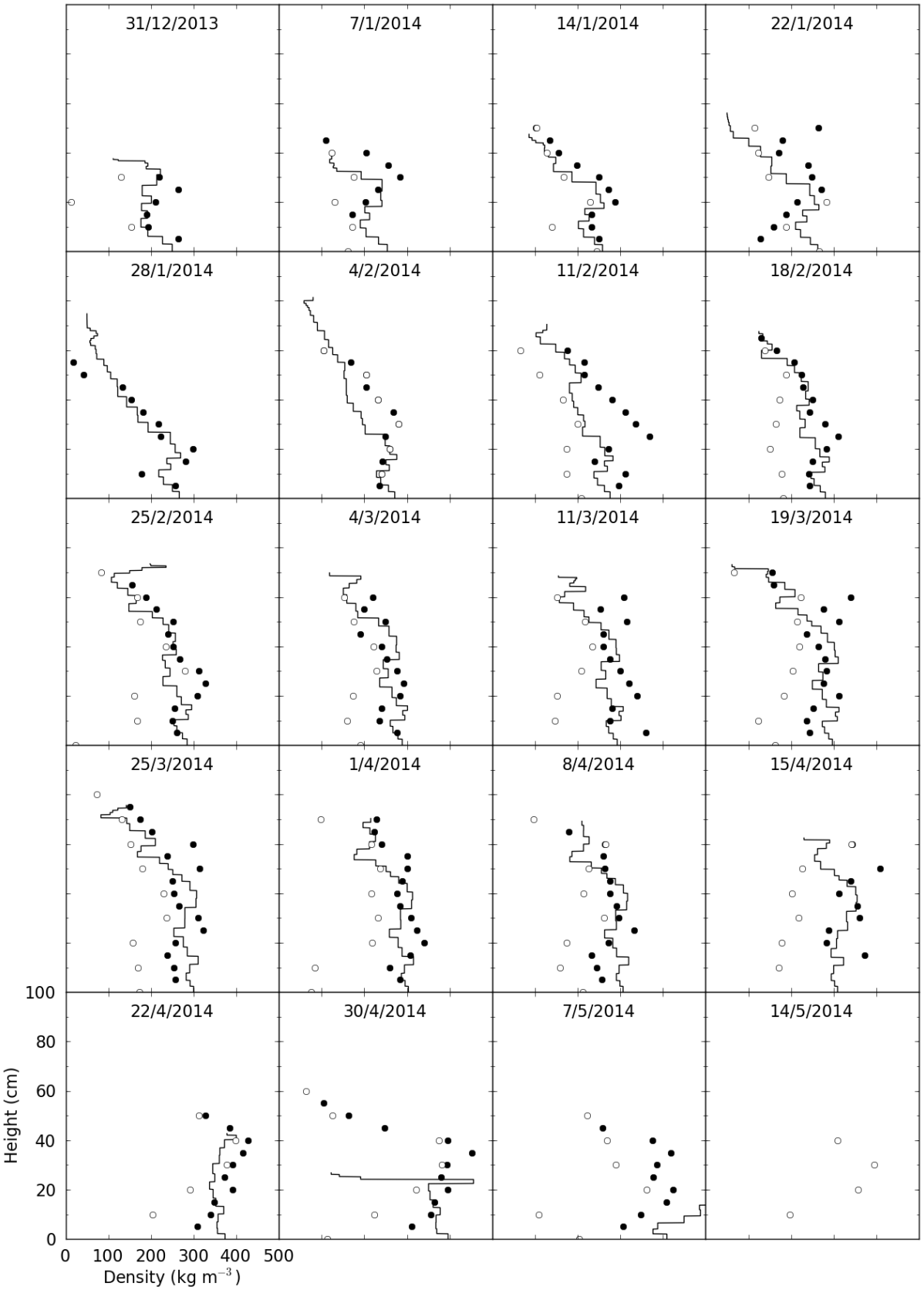

Figure S3. Profiles of snow temperature from manual measurements (black dots), thermistors (white dots) and Crocus simulations (lines).

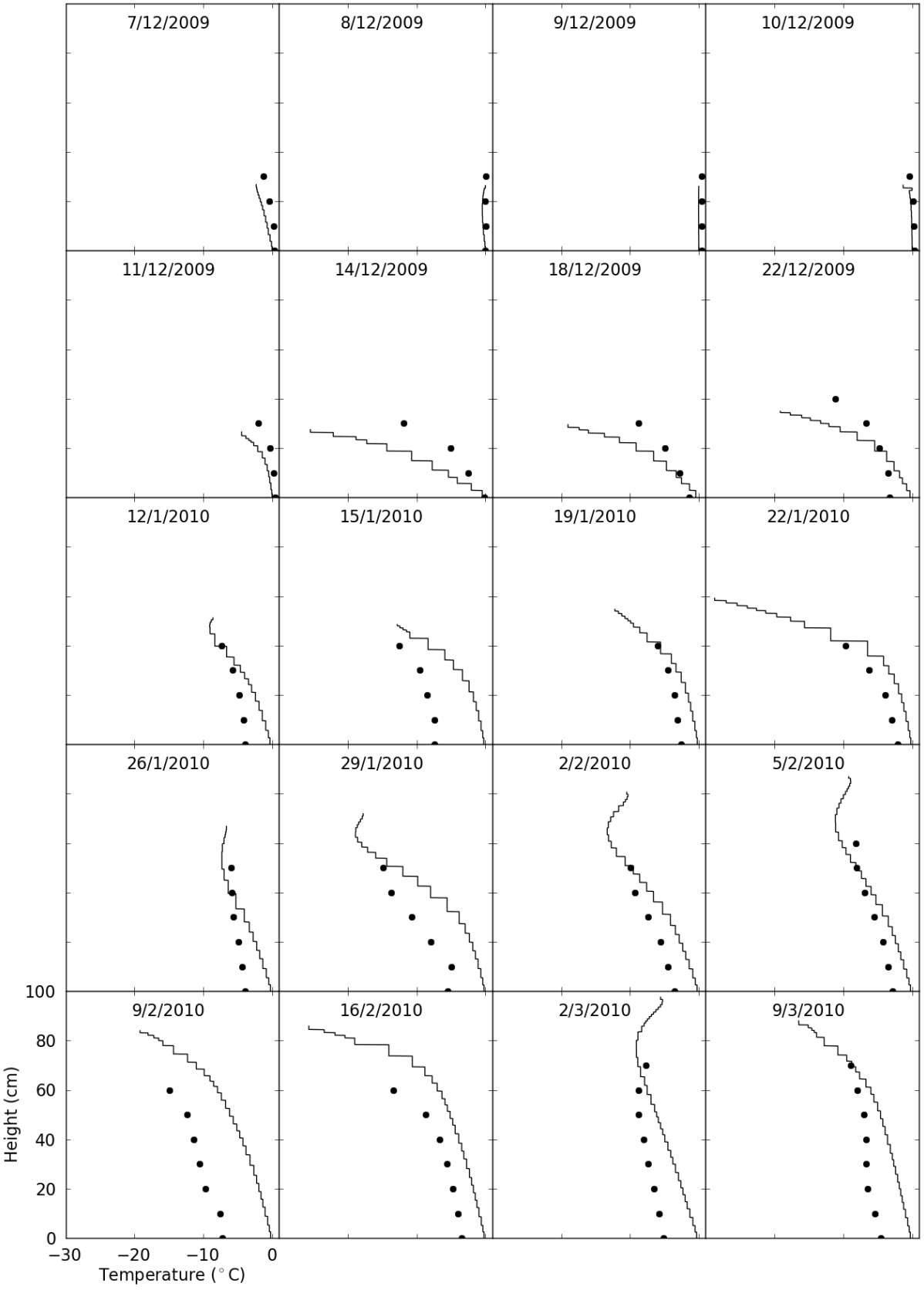

Figure S3. Continued

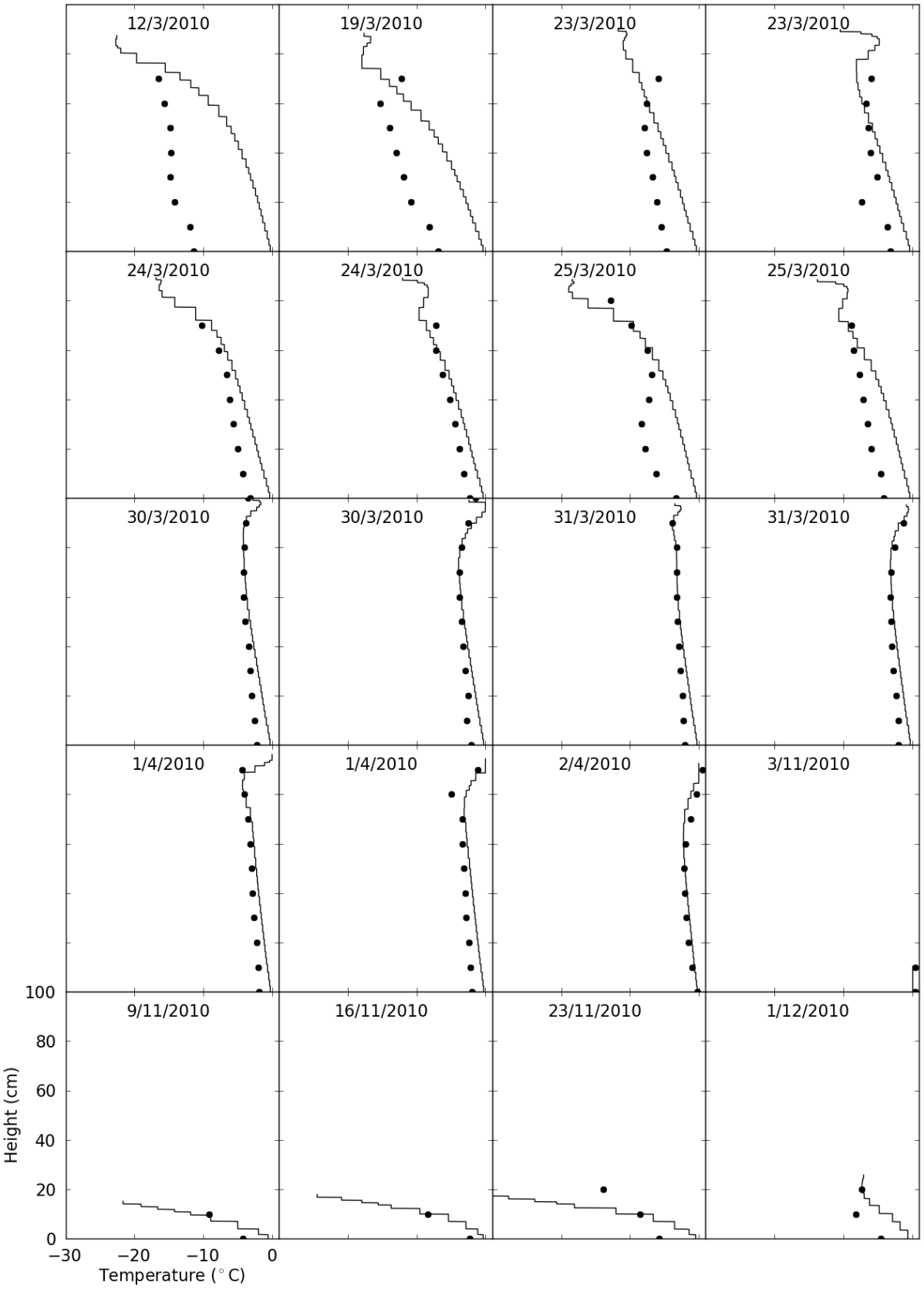

Figure S3. Continued

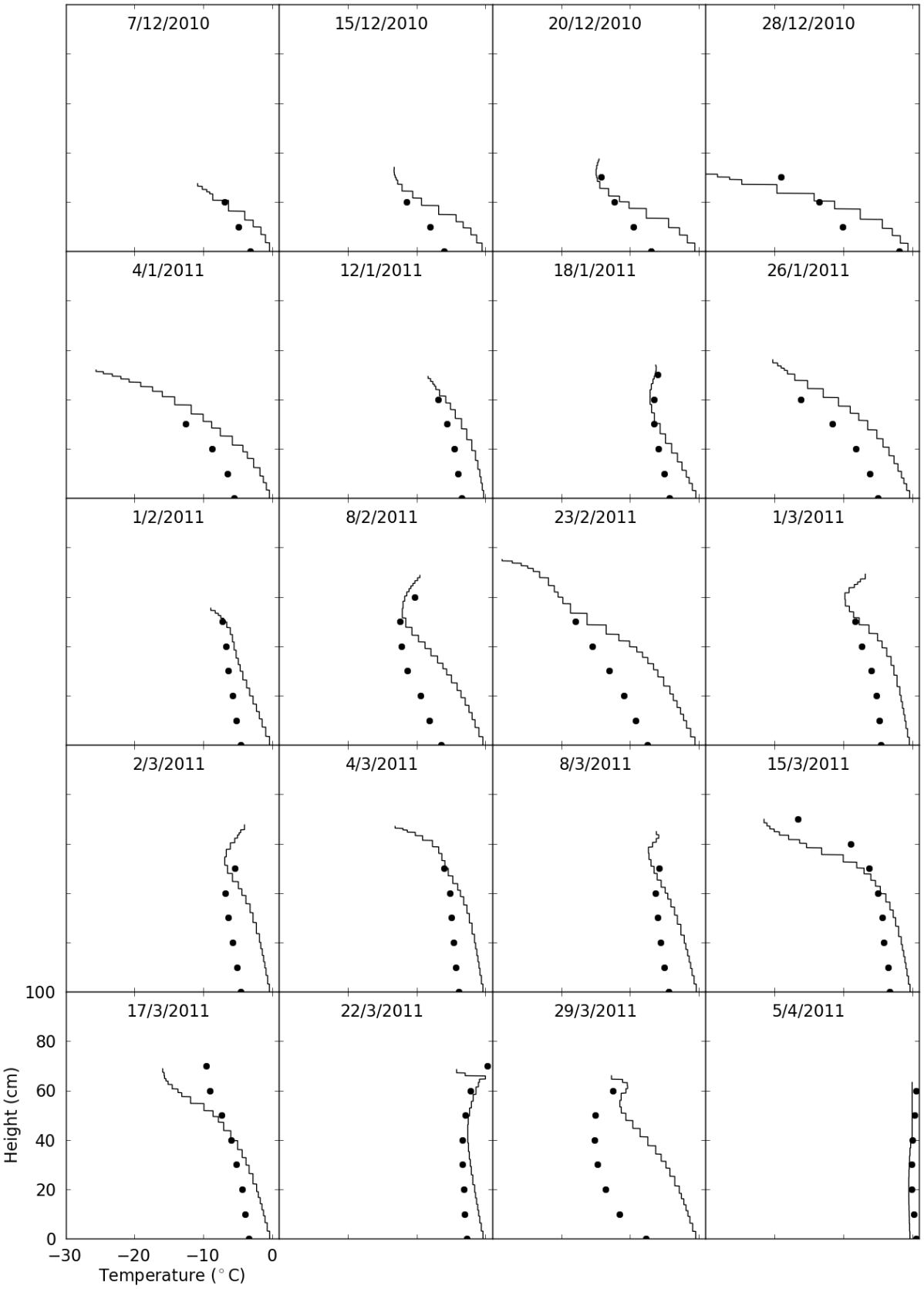

Figure S3. Continued

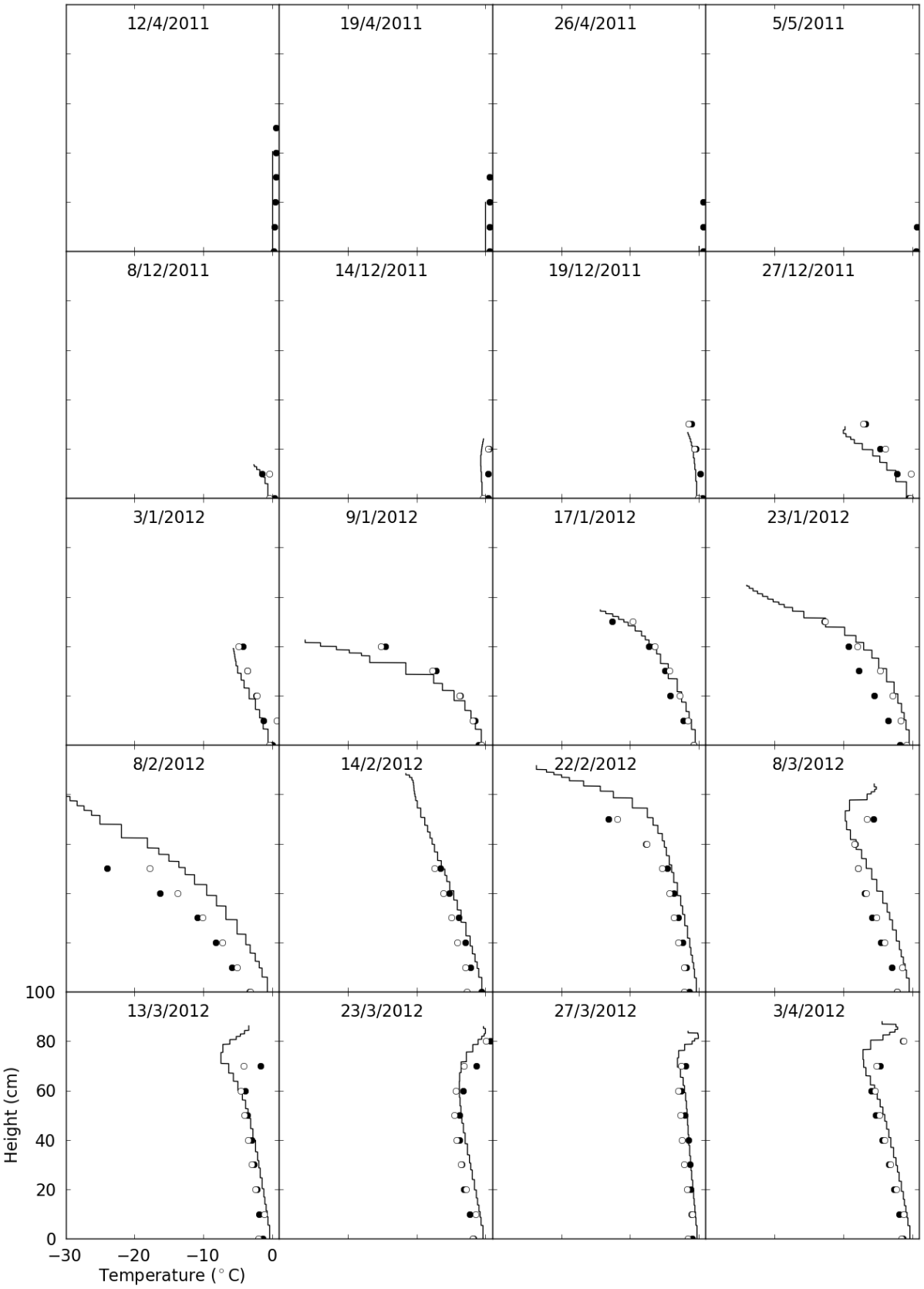

Figure S3. Continued

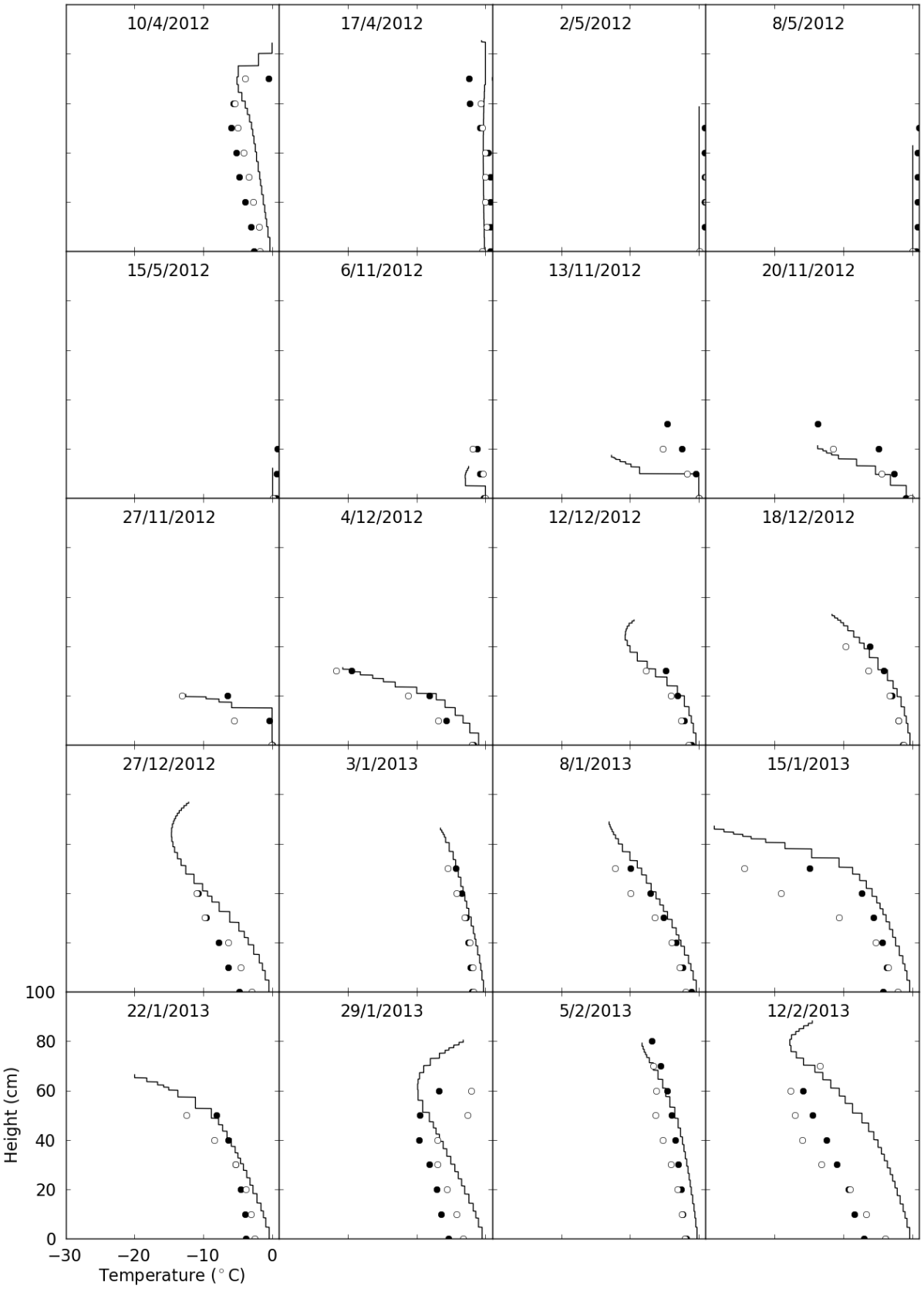

Figure S3. Continued

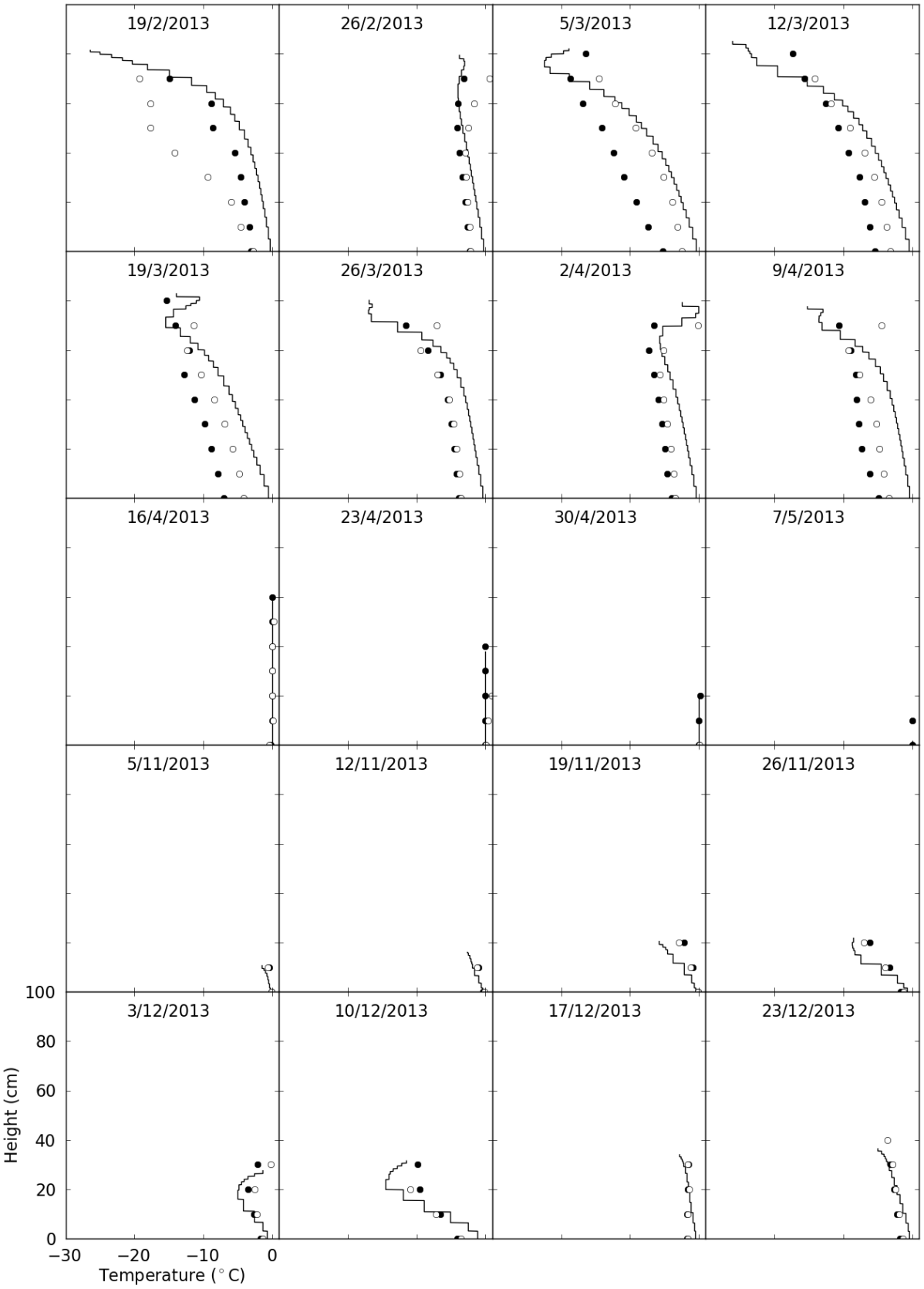

Figure S3. Continued